

# Atomic simulation of the 30° partial dislocation interaction with divacancy in silicon

Chaoying Wang\* and Qingyuan Meng

Department of Astronautical Science & Mechanics, Harbin Institute of Technology, P.O. Box 344, Harbin, 150001, P.R. China

Received 25 November 2008, revised 24 January 2009, accepted 26 January 2009

Published online 2 February 2009

PACS 61.72.Bb, 61.72.jd, 61.72.Lk, 71.15.Pd

\* Corresponding author: e-mail chaoyingwang@gmail.com, Phone: +86 045186414143, Fax: +86 045186221048

The interactions of the 30° partial dislocation with a divacancy ( $V_2$ ) in silicon are investigated by the molecular dynamics simulation method. The results under different temperature and shear stress conditions show that the 30° partial dislocation is pinned when the dislocation encounters  $V_2$ . When the shear stress approaches a critical value  $\tau_c$ , the dis-

location can overcome the pin. As the temperature increases,  $\tau_c$  decreases approximately as a linear function. Moreover, it is found that  $\tau_c$  is mainly determined by the migration barrier of the corresponding kink. Finally,  $V_2$  can make the 30° partial dislocation move faster once the dislocation overcomes the pin.

© 2009 WILEY-VCH Verlag GmbH & Co. KGaA, Weinheim

**1 Introduction** Divacancy ( $V_2$ ) and dislocation are the fundamental defects in silicon and other semiconductors.  $V_2$  is particularly attractive from the experimental point of view because it can be easily produced by electron irradiation and is quite stable and immobile. For the dislocation, it is not only related to plastic deformation behavior, but also concerned with electronic and optical properties of electronic devices. Thus, the mobility of dislocations attracted much interest in the past years [1–3]. But most of these studies were concerned with pure Si crystal without considerations of other defects. In view of actual physical phenomena, the vacancies cannot be ignored in the dislocation migrations. In fact, some earlier experiments indicate that the vacancies may change the dislocation migration properties [4–6]. The interactions of vacancies with dislocations have been studied by Justo et al., but they mainly focused on the formation energies of vacancies in the stacking fault (SF) and dislocation cores [7, 8]. For the underlying dynamic details of interaction between dislocation and vacancies, little is known on the atomic level.

There is a consensus that the dislocation mobility in silicon is dominated by the 30° partial dislocation [9]. It orientates along  $\langle 110 \rangle$  and glides in the  $\{111\}$  plane [10, 11]. Due to the high Peierls barrier in Si, the dislocation movement is induced by the nucleation and migration of

kinks along the dislocation line [11]. In the reconstructed 30° partial dislocation, there are four kinds of kinks: left kink (LK), right kink (RK), LK-reconstruction defect complex (LC), and RK-reconstruction defect complex (RC) [2]. The microstructures of the four kinks are shown in Fig. 1. It can be seen that the interactions of dislocations with vacancies turn to be kink interactions with vacancies.

In this letter, we choose the stable and immobile  $V_2$  to interact with the 30° partial dislocation during the dislocation migration processes. By performing a series of molecular dynamics (MD) simulations over a range of temperature and shear stress, the interaction processes are described. In addition, the influences of  $V_2$  on the 30° partial dislocation migration properties are explained on the atomic level.

**2 Simulation method** The efficient tool to study dislocation migration in detail is the MD method together with empirical potentials, which can conduct tens of thousands of atoms for a long time period. It is found that the Stillinger–Weber (SW) potential [12] can be used to describe the configuration and calculate the energy of 30° partial dislocations [13]. Moreover, it has been proved to be the best empirical potential under large shear stress [14]. Thus, SW is employed in this work. The MD simulations

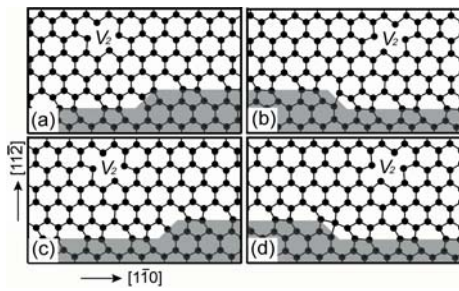


**Figure 1** Atomic configurations of the four kinks and  $V_2$ . (a) Left kink (LK) and  $V_2$ . (b) Right kink (RK) and  $V_2$ . (c) LK-reconstruction defect complex (LC) and  $V_2$ . (d) RK-reconstruction defect complex (RC) and  $V_2$ . The shaded areas indicate the stacking fault.

are carried out under the *NPT* ensemble, which means that the particle number  $N$ , pressure  $P$  and temperature  $T$  are kept constant. The periodic boundary conditions (PBCs) are adopted in all three dimensions and the time step for all simulations is 1 fs.

Each model is constructed for the four kinks shown in Fig. 1. For LK and RC, the three vectors are  $6[111]$ ,  $20[11\bar{2}]$  and  $21.5[1\bar{1}0]$ , containing 31413 atoms. For RK and LC, the three vectors are  $6[111]$ ,  $20[11\bar{2}]$  and  $20.5[1\bar{1}0]$ , containing 29520 atoms. In each model, two dislocations separated by  $10[11\bar{2}]$  with opposite Burgers vectors are formed in the  $\{111\}$  plane, giving zero net Burgers vectors and allowing the use of PBCs in all three dimensions as well. The shortcomings of the dislocation dipole method are that we should consider the interaction between the two dislocations and the interactions between the dislocation dipole and its images due to the PBC. In order to test the sensitivity of results to the interactions, simulations for the bigger models  $12[111]$ ,  $30[11\bar{2}]$ ,  $31.5[1\bar{1}0]$  (LK and RC) and  $12[111]$ ,  $30[11\bar{2}]$ ,  $30.5[1\bar{1}0]$  (RK and LC) are conducted. Compared with the above small models, the excess energies per unit length of dislocation agree within 0.2%. This means that these interactions caused by the dipole and PBC are small enough to be neglected.

$V_2$  is formed by removing two adjacent atoms near the kink in each model. Then the systems are relaxed for 10000 steps at 0 K and stable configurations are obtained as shown in Fig. 1.

**3 Results and discussion** A series of MD simulations are conducted for each of the four kink species to thoroughly investigate the interaction between 30° partial dislocations and  $V_2$ . In consideration of the fact that LK may produce one or more kink pairs and RK may dissociate into RC + reconstruction defect structures when the temperature is higher than 1000 K [2], hence the temperature is set from 800 K to 1000 K by a step interval of 50 K. Under the constant temperature conditions, an external shear stress is applied by means of the Parrinello–Rahman method [15] to make the dislocation move. In this work, the shear stress direction is along the Burgers vector of the 30° partial dislocation. Due to the high Peierls barrier of Si, the calculation

starts from 2.5 GPa and increases at a step interval of 0.025 GPa until the dislocation overcomes the pin of  $V_2$ . The time of each calculation amounts to 450 ps and the configurations of models are recorded at a time step of 0.1 ps.

Under constant temperature and shear stress, the kinks in the initial states shown in Fig. 1 are moving to the left (LK and LC) and right (RK and RC). In Fig. 2a, the dislocation encounters  $V_2$  and is pinned.  $V_2$  breaks the dislocation into two segments, each having one rooted in the vacant sites and one free end on the side of the model. Due to the external shear stress, the free ends and arms are still moving. In this process, the dislocation stretches and forms the V-character shape shown in Fig. 2b. If the shear stress is not big enough to overcome the pin of  $V_2$ , the two free arms will still move until they encounter each other. Figure 2c is the picture that the two segments of the pinned 30° partial dislocation encounter in the  $\{111\}$  plane. Because  $V_2$  is not formed in the middle of the dislocation direction, the two segments are not equal to each other, which results in that the encountered two parts are not perpendicular to the  $Z$  direction.

In the Fig. 2b condition, if the shear stress is raised, there exists a critical value at which the dislocations can overcome the pin of  $V_2$ . This critical shear stress is recorded as  $\tau_c$ . After the dislocation is released, the pinned part begins to move with the free segments. It is important to note that the dislocation energy increases with the stretching of the dislocation line shown in Fig. 2b. Thus, there exists a recovery stress in the dislocation line. Once the dislocation overcomes the pin of  $V_2$ , the pinned part will move faster than the two free segments under the action of external stress and the recovery stress. This process is shown in Fig. 2d.

The  $\tau_c$  of LK, RK, LC and RC under different temperatures are listed in Fig. 3. It can be seen that  $\tau_c$  decreases approximately as a linear function of temperature. This can be explained that the dislocation may become more energetic to overcome the pin due to the increase of temperature, which results in a decrease of  $\tau_c$ . On the other hand, the migration ability of kinks in the 30° partial dislocation

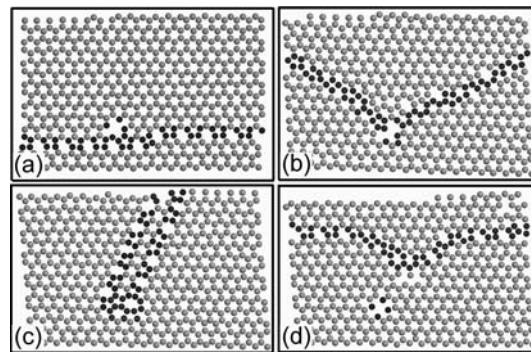


**Figure 2** Schematic view of the interaction processes between 30° partial dislocation and  $V_2$ . (a) → (b) → (c): The process of dislocation is pinned by  $V_2$ . (a) → (b) → (d): The process of dislocation overcomes the pin of  $V_2$ .

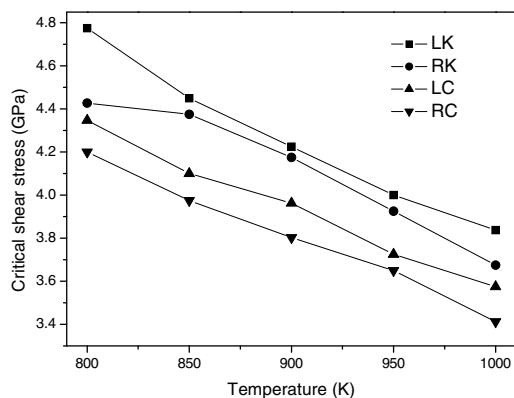


**Figure 3** Critical shear stress ( $\tau_c$ ) of LK, RK, LC and RC under different temperature conditions.

is controlled by their migration barriers [3, 9]. It is found that the migration barriers are RC (1.12 eV) < LC (1.82 eV) < RK (2.29 eV) < LK (2.84 eV) [2], which results in that  $\tau_c$  (RC) <  $\tau_c$  (LC) <  $\tau_c$  (RK) <  $\tau_c$  (LK) under the same temperature condition in Fig. 3. This also indicates that  $\tau_c$  is mainly determined by the migration barrier of kinks.

To investigate the influence of  $V_2$  to the migration properties of  $30^\circ$  partial dislocations, we conduct comparative calculations in the model with and without  $V_2$  under 1000 K and 4 GPa conditions. Under shear stress, the kinks begin to move from the same position of the models. When the dislocations arrive at similar positions, the time and final atomic configurations are as shown in Fig. 4. It can be seen that a dislocation in the model without  $V_2$  (upper panel) uses more time than in the model with  $V_2$  (lower panel) for the same kink. This means that if the  $30^\circ$  partial dislocation can overcome the pin, it will move faster. One possible explanation may come from the additional recovery stress. The kinks move under external shear stress in the model without  $V_2$ . But when the dislocation overcomes the pin in the model containing  $V_2$ , besides the external shear stress, the additional recovery stress will make it

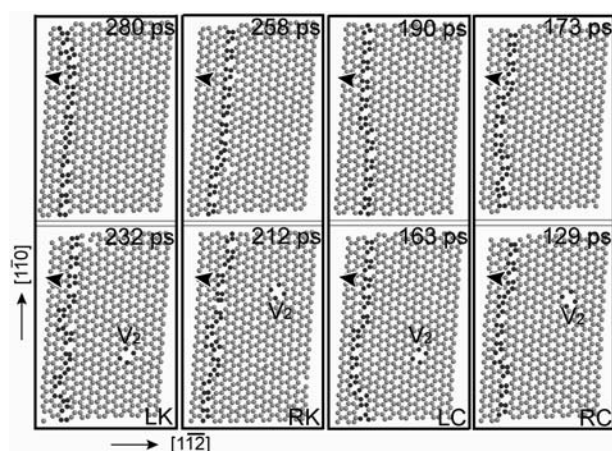


**Figure 4** Atomic constructions and the time that dislocations move to similar positions in the models without (upper panel) and with  $V_2$  (lower panel).

move faster. On the other hand, the migration processes of kinks are carried out by bond breaking, rotation and forming [2]. Dislocations in materials generate a strain field. The existence of  $V_2$  provides more space for strain relaxation and four dangling bonds as well, which make the bonds break and rotate easily. Moreover, the dangling bonds provide more possibilities for the dislocation to form kinks. The more kink structures in the lower panel of Fig. 4 have validated this opinion. In these conditions, the dislocation will obviously move faster than in the model which has only one kink in the dislocation line.

**4 Conclusions** In summary, we particularly described the interactions of  $V_2$  with a  $30^\circ$  partial dislocation. It is found that the  $30^\circ$  partial dislocation is pinned when the dislocation encounters  $V_2$ . When the shear stress increases to a critical value  $\tau_c$ , the dislocation overcomes the pin and moves continuously.  $\tau_c$  decreases approximately as a linear function of temperature. Moreover, the corresponding abilities to overcome the pin are determined by the migration barriers of kinks. Finally, because of the existence of  $V_2$ , an additional recovery stress and more kink structures make the  $30^\circ$  partial dislocation move faster after it has moved through  $V_2$ .

**Acknowledgement** This work is supported by the National Natural Science Foundation of China (Grant No. 10772062).

## References

- [1] V. V. Bulatov, S. Yip, and A. S. Argon, *Philos. Mag. A* **72**, 453 (1995).
- [2] C. Y. Wang, Q. Y. Meng, K. Y. Zhong, and Z. F. Yang, *Phys. Rev. B* **77**, 205209 (2008).
- [3] N. Oyama and T. Ohno, *Phys. Rev. Lett.* **93**, 195502 (2004).
- [4] S. W. Lee, H. C. Chen, L. J. Chen, Y. H. Peng, C. H. Kuan, and H. H. Cheng, *J. Appl. Phys.* **92**, 6880 (2002).
- [5] E. A. Stach, R. Hull, J. C. Bean, K. S. Jones, and A. Nejim, *Microsc. Microanal.* **4**, 294 (1998).
- [6] R. Hull, E. A. Stach, R. Tromp, F. Ross, and M. Reuter, *Phys. Status Solidi A* **171**, 133 (1999).
- [7] J. F. Justo, M. Koning, W. Cai, and V. V. Bulatov, *Phys. Rev. Lett.* **84**, 2172 (2000).
- [8] J. F. Justo, M. Koning, W. Cai, and V. V. Bulatov, *Mater. Sci. Eng. A* **309**, 129 (2001).
- [9] H. R. Kolar, J. C. H. Spence, and H. Alexander, *Phys. Rev. Lett.* **77**, 4031 (1996).
- [10] M. S. Duesbery and G. Y. Richardson, *Crit. Rev. Solid State Mater. Sci.* **17**, 1 (1991).
- [11] J. P. Hirth and J. Lothe, *Theory of Dislocations*, second ed. (Wiley, New York, 1982).
- [12] F. H. Stillinger and T. A. Weber, *Phys. Rev. B* **31**, 5262 (1985).
- [13] M. S. Duesbery, B. Joos, and D. J. Michel, *Phys. Rev. B* **43**, 5143 (1991).
- [14] J. Godet, L. Pizzagalli, S. Brochard, and P. Beauchamp, *J. Phys.: Condens. Matter* **15**, 6943 (2003).
- [15] M. Parrinello and A. Rahman, *Phys. Rev. Lett.* **45**, 1196 (1980).